Macromolecules

ARTICLE

pubs.acs.org/Macromolecules

Lubrication Mechanism of Concentrated Polymer Brushes in Solvents: Effect of Solvent Quality and Thereby Swelling State

Akihiro Nomura,[†] Kenji Okayasu,[†] Kohji Ohno,[†] Takeshi Fukuda,[†] and Yoshinobu Tsujii[†,‡,*]

[†]Institute for Chemical Research, Kyoto University, Uji, Kyoto 611-0011, Japan

[‡]JST, CREST, Uji, Kyoto 611-0011, Japan

ABSTRACT: The lubrication mechanism of concentrated polymer brushes (CPBs) exhibiting ultralow frictional property was investigated. The frictional force and hence the frictional coefficient μ between CPBs of polystyrene (PS) were measured as a function of shear velocity v and degree of swelling. The degree of swelling was precisely controlled by varying the composition of solvent , which consisted of a mixture of toluene (good solvent for PS) and 2-propanol (nonsolvent for PS), from the brush highly stretched state (toluene rich) to glassy state (2-propanol rich). The μ data of the mixtures revealed two lubrication mechanisms, i.e., boundary and hydrodynamic lubrication. Boundary lubrication with μ values less dependent on shear velocity was observed both in ultralow (μ on the order of 10^{-4}) and high frictional (μ on the order of 0.1) regimes. On the other hand, hydrodynamic lubrication was well described by the relation $\mu = \beta \cdot v^{\alpha}$ with α having an almost constant value of ca. 0.7. It was found that parameter β depended on the solvent composition and was scaled by the degree of swelling. It should be noted that the confronted polymer brushes interacted with each other even in this regime. Thus, CPBs in solvents may be employed as an efficient lubricating layer due to their unique features.

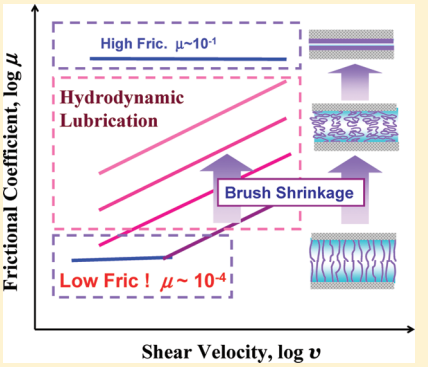

INTRODUCTION

The frictional/lubrication property of polymer-coated surfaces is an important characteristic in many areas of science and technology.[1−3] Polymer brushes, in particular, have been extensively studied because of their efficiency at modifying the equilibria and dynamic properties of surfaces.[4−11] They have been shown to be an efficient lubricant and wet layer at moderate shear velocities and loads.[8−11] Previously, well-defined polymer brushes were prepared from end-functionalized polymers or block copolymers with the terminal group or one of the blocks selectively adsorbed onto a surface. These systems possess rather low graft densities of typically 0.001−0.05 chains/nm^2, corresponding to the "semidilute polymer brush (SDPB)" regime, which limits their application to the preparation of a brush layer thick enough to hold a wide range of pressure and shear velocity for practical use.

In recent studies, we have succeeded in densely grafting well-defined polymers on various kinds of materials including inorganic substrates using the living radical polymerization technique.[12−14] The graft density of thus obtained polymer brushes was about an order of magnitude higher than those of typical SDPBs, penetrating deep into the regime of "concentrated polymer brush (CPB)", which had been little explored systematically because of the unavailability of such brush samples. Recent studies revealed that these CPBs have structures and properties quite different and even unpredictable from those of SDPBs: most strikingly, CPBs of poly(methyl methacrylate) (PMMA) swollen in a good solvent (toluene) exhibit equilibrium film thicknesses as large as 80%−90% of the full (contour) length of the graft chains.[15,16] More interestingly, the microtribological analysis using an atomic force microscope (AFM) revealed that in a good solvent, CPBs of PMMA exhibit super lubrication with an extremely low frictional coefficient ($\mu \sim 10^{-4}$) for any applied load.[17] Other examples of polymer brushes with excellent lubrication properties have been reported for SDPBs of polyelectrolyte and for a polyzwitterionic brush (whose graft density was not reported).[9] The excellent water-lubrication characteristics were ascribed to the osmotic pressure of counterion and the strong hydration of charged groups. In contrast, we previously attributed the super lubrication observed for the swollen CPBs of PMMA to the strong resistance of CPBs against mixing with each other: that is, confronted CPBs (of the same kind) do not mix with each other at high compression. This new mechanism was expected to be common to CPB/good solvent systems.

Parallel to our studies, Kobayashi et al. studied the tribological properties of densely grafted polymer brushes of various polymers using a tribometer with a probe ball 5 mm in diameter.[18−21] They revealed lower frictional forces and improved wear resistance as compared with the corresponding spin-cast polymer film. The frictional coefficient μ for these systems was not of the same value reported above; the discrepancy may be attributed to the different experimental conditions employed. Microtribological measurements are suitable for revealing the intrinsic frictional/lubrication properties of solvent-swollen polymer brushes with, for example, submicrometer thickness.

Received: February 19, 2011
Revised: April 20, 2011
Published: May 19, 2011

Table 1. Characteristics of PS-Brush Samples

sample	M_n	M_w/M_n	L_d/nm	σ /chains nm^{-2}	σ^*
1	34 000	1.29	25	0.46	0.30
2	38 000	1.19	26	0.44	0.29
3	37 000	1.27	29	0.49	0.32
probe	33 000	1.17	-	-	-

As mentioned above, CPB successfully achieved super lubrication. The solvent-swollen polymer brush can be regarded as a thin lubricating layer. Concerning the fluid character of the brush layers, the thickness and viscosity of the lubricating layer and the shear velocity should affect the frictional/lubrication property.[22] However, these effects warrant further investigation. In this work, AFM-microtribological studies were carried out on well-defined CPBs of polystyrene (PS) under varying degrees of swelling, which was precisely controlled by changing the composition of good/poor-solvent mixtures. The lubrication mechanism of CPBs is discussed in detail in terms of hydrodynamic and boundary lubrications. We believe that this is the first time that such an in-depth analysis has been presented.

EXPERIMENTAL SECTION

Materials. Styrene (99%, Nacalai Tesque, Inc., Japan) was passed through a column of basic alumina to remove inhibitors. Cu^{I}Br (99.9%, Wako Pure Chemical Ind., Ltd., Japan), ethyl 2-bromoisobutylate (EBIB, 99%, Wako), and 4,4′-dinonyl-2,2′-bipyridine (dNbipy, 97%, Aldrich) were used as received. (2-bromo-2-methyl) propionyloxyhexyltriethoxysilane (BHE, a fixable initiator for ATRP) was prepared as previously reported.[23] All other reagents were obtained from commercial source and used as received.

A silicon wafer (Ferrotec Corp., Japan, one side chemical/mechanical polished, 525 μm thickness) was cleaned by ultrasonication in $CHCl_3$ for 15 min and ultraviolet (UV)/ozone treatment for 10 min before fixation of BHE. A silica particle (SiP, HIPRESICA SP, radius R of 5 μm) used as a probe for the AFM measurement was obtained from Ube Nitto Kasei Co., Ltd., Japan.

Synthesis of Concentrated PS Brushes via Surface-Initiated ATRP. Well-defined CPBs of PS were prepared by surface-initiated ATRP. To immobilize the surface initiator, BHE, a silicon wafer was immersed in an ethanol solution containing BHE (1 wt %) and 28%-aqueous ammonium (5 wt %) for 12 h at room temperature, copiously rinsed with ethanol, and then dried. The BHE-immobilized silicon wafer was subjected to graft polymerization at 110 °C for 2 h in a styrene solution containing Cu(I)Br (87 mM), dNbipy (170 mM), and EBIB (8.7 mM) under argon atmosphere. EBIB was added as a free initiator not only to control the polymerization by the so-called persistent radical effect but also to yield free polymers, which are useful as a measure of the molecular weight M_n and molecular weight distribution M_w/M_n of the graft chains.[13] Good agreement in M_n and M_w/M_n between the graft and free polymers has been reported by several research groups including us.[24−29] After polymerization, the substrate was rinsed in a Soxhlet extractor with toluene for 8 h to remove physisorbed polymers and impurities. The thickness L_d of the polymer layer in a dry state was determined by ellipsometry (M-2000U, J. A. Woolam, Lincoln, NE). The characteristics of the PS brushes are summarized in Table 1. The number-average molecular weight, M_n, and the polydispersity index, M_w/M_n, are those of the free polymer analyzed by gel permeation chromatography (GPC). The graft density σ was calculated from the determined values of M_n and L_d by the following equation $\sigma = \rho L_d N_A/M_n$, where ρ is the bulk density of a PS film (=1.05 g/cm^3)[30] and N_A is Avogadro constant. As a good measure of graft density for various kinds of polymer brushes, the surface occupancy, σ^*, was defined as $\sigma^* = s_c\,\sigma$, where s_c is the cross-sectional area per monomer unit given by $s_c = v_0/l_0$ with v_0 being the molecular volume per monomer unit (estimated from bulk density of monomer in this case) and l_0 being the chain length per monomer unit (l_0 = 0.25 nm for vinyl polymers).

The PS brush was also fabricated on the SiP as described above. The SiP was dispersed by 0.5 wt % in the BHE solution, magnetically stirred for 12 h at room temperature, and then solvent-exchanged to styrene, to afford a 0.5 wt %-SiP dispersion that was then subjected to ATRP of styrene. Finally, the PS-grafted SiP was copiously washed with chloroform.

AFM Measurements. The degree of swelling of a polymer brush in a solvent was estimated by force measurements and scratched groom imaging on an AFM (Seiko Instruments Inc., Japan, SPI3800 controller with SPA400 unit). This procedure has been described in detail elsewhere.[15,16] A V-shaped cantilever OMCL-TR800 (Olympus Corp., Japan, normal spring constant k_n = 0.15 N/m) was used with a bare (unmodified) SiP probe attached using a two-component epoxy−resin adhesive. The R of the probe particle was 5.0 μm, much larger than the size of graft layer so that the graft chains could be viewed as being compressed by a flat surface. A liquid cell was used for the measurement in mixtures of toluene and 2-propanol with different compositions (f_{TOL}, volume fraction of toluene). The mixed solvents were filtered through a cellulose porous membrane (Whatman, diameter 0.1 μm) before use. The normal displacement Δz of the cantilever was monitored as a function of separation in approaching/retracting modes; typically, an approaching/retracting speed of 80 nm/s, and at least 8 force curves were taken at different locations. The interaction force, i.e., the normal force, F_n, was estimated as follows,

$$F_n = k_n \Delta z = k_n(\mathrm{DIF}\cdot S_{\mathrm{DIF}}) \quad (1)$$

where DIF (V) and S_{DIF} (m/V) are the signal intensity and sensitivity of the vertical deflection, respectively. The latter value was determined for each force curve in the so-called constant-compliance region where the cantilever deflection increased linearly with decreasing separations. The AFM raw data of cantilever deflection vs displacement were converted into F_n as a function of separation D' according to the principle of Ducker et al.[31] The separation D' is not the distance from the substrate but that from the constant-compliance region. In a system with a dense polymer layer, the distance between $D' = 0$ plane and the substrate surface, which is called as "offset distance D_0" can be very large. We measured the offset distance D_0 by AFM-imaging under a constant force mode by applying the force corresponding to the constant compliance region in the force measurements. The true distance D between the surfaces of the substrate and the probe sphere was defined as $D = D' + D_0$. The determination of D_0 and hence D in each solvent condition gives the equilibrium thickness L_e of the brushes in solvent, where L_e is the critical true distance at a repulsive force onset (0.05 nN was employed as onset value of F_n).

The frictional measurement was performed by the so-called force curve method. The same procedures outlined above were employed unless otherwise stated. The PS-brush-grafted SiP was mounted on a rectangular-shaped cantilever OMCL-RC800 (Olympus, k_n = 0.1 N/m) for the friction measurement. The lateral displacement Δx as well as Δz of the cantilever were simultaneously monitored in approaching/retracting modes, while the substrate was slid back and forth in the horizontal plane normal to the cantilever by applying a triangular-wave oscillation on a piezo actuator via a function generator (Wave Factory 1945, NF Corp, Japan). The normal and frictional forces (F_n and F_s) were evaluated according to eqs 1 and 2, respectively.

$$F_s = k_s \Delta x = k_s(\mathrm{FFM}\cdot S_{\mathrm{FFM}}) \quad (2)$$

where k_s, FFM (V), and S_{FFM} (m/V) are the torsional spring constant of the cantilever, the signal intensity and sensitivity of the torsional deflection, respectively. The torsional-deflection sensitivity was estimated

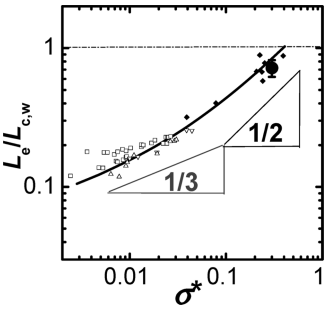

Figure 1. Plot of degree of stretching $L_e/L_{c,w}$ vs dimensionless graft density σ^* of the PS brush (sample 1) in toluene (●). Other symbols reprocessed from ref 16 show the data for some other polymer brushes in good solvents including the CPB of PMMA in toluene (small closed symbols).

from S_{DIF} by correcting the difference in geometry of the reflected-light path ($L/2R$) and amplification factor of the detectors, where L is the cantilever length.[32] The k_s was calculated to be 23 N/m using the following equation[33]

$$k_s = GWT^3/3L \quad (3)$$

where G, W, and T are the shear modulus, width, and thickness of the cantilever, respectively. For some selected levers, the commercially reported k_n and above-calculated k_s values were experimentally found to have an error of 10% and 20%, respectively, by the resonant technique.[34] The observed signal proportional to Δx was modulated by the reciprocal motion. Thus, the signal was processed through a high-pass filter (Multifunction filter 3611, NF Corp., Japan) to remove a lower-frequency component, which is mainly caused by vertical deflection of the cantilever, and finally converted to the FFM data as the root-mean-square value with AC-volt meter (M2170, NF Corp, Japan). Typically, the approaching/retracting speed and the distance of shearing was set to be 27 nm/s and 1 μm, respectively, and 4 force curves were recorded and averaged at different locations for each measurement. The shear velocity v (4−1000 μm/s) was changed by adjusting the oscillating frequency (2−500 Hz). The distance of shearing was calibrated by AFM-observations of the scratched trace on a bare silicon wafer with a harder cantilever OMCL-AC160TS (Olympus, k_n = 42 N/m).

The F_s was also measured by the so-called "frictional-loop" method, in which the torsion of the cantilever was monitored during repeated reciprocal/lateral movement of the piezo with a constant F_n. The distance of shearing was 5 μm, and the shear velocity (4−1000 μm/s) was changed by adjusting the shearing frequency (0.4−100 Hz).

The frictional coefficient was defined as $\mu = F_s/F_n$.

RESULTS AND DISCUSSION

Swelling in Mixed Solvents. Scaling theoretical analysis predicted that the L_e of polymer brushes in good solvent varies with $L_e \propto L_c \sigma^{*\alpha'}$, where L_c is the contour length of the graft chain and the α' value is $^1/_3$[35,36] and $^1/_2$[37,38] for SDPB and CPB, respectively. We successfully measured the L_e as a function of graft density for the brushes of PMMA in good solvent and determined the crossover density between SDPB and CPB to be around 0.1 for σ^* using, e.g., a combinatorial method. Figure 1 shows the plot of $L_e/L_{c,w}$ vs σ^* in logarithmic scale, where $L_{c,w}$ is the contour length of the graft chain calculated from the M_w value. The data for the present samples in toluene were compared with those for various kinds of polymer brushes including the CPB of PMMA previously studied in toluene. The present samples had a σ^* value sufficiently higher than the above-mentioned criterion, and the graft chains were highly stretched, similar to the previous results of CPB of PMMA in a good solvent. Thus, the prepared samples can be justifiably categorized as belonging to the CPB regime.

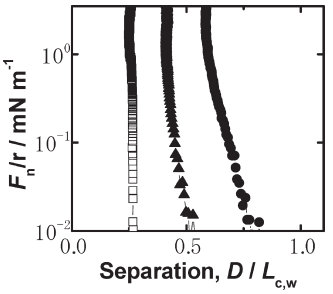

Figure 2. Force curves of the PS brush (sample 1) measured in toluene/2-propanol-mixed solvents with different compositions; f_{TOL} = 0.0 (□), 0.5 (▲), 1.0 (●). The bare SiP (R = 5 μm) mounted on triangular-shaped cantilever was used as a probe.

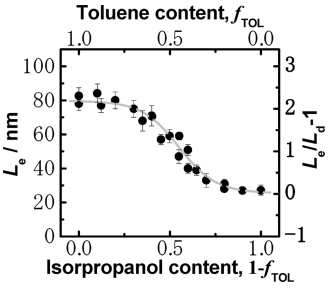

Figure 3. Plots of equilibrium thickness L_e and swelling ratio $L_e/L_d - 1$ of the PS brush (sample 1) in toluene/2-propanol-mixed solvents. The gray curve is the result fitted with sigmoid function.

Figure 2 shows the force curves of the CPB of PS against the bare SiP probe in solvents with f_{TOL} = 1 (pure toluene), 0.5, and 0 (pure 2-propanol). It should be noted that the horizontal axis in this figure was corrected to the true distance D between the surfaces of the base substrate and the probe sphere, thus corresponding to the thickness of the PS-brush layer if F_n is detected. In toluene (at f_{TOL} = 1.0), the equilibrium thickness L_e, defined as the maximum distance with F_n detectable, reached 80% of the $L_{c,w}$. This force curve indicates not only high stretching of chains but also strong resistance of compression as F_n steeply increases. This is one of the most important properties of CPB in good solvents. Figure 2 suggests that with decreasing f_{TOL} and hence decreasing the solvent quality, the PS brush increasingly shrank. Details are shown in Figure 3 as plots of L_e and $L_e/L_d - 1$ as a function of f_{TOL}, where the value of $L_e/L_d - 1$ gives the volume fraction of solvent absorbed in the polymer-brush layer. When $f_{TOL} > 0.8$, the solvent quality was sufficiently good to promote high extension of the chains of the polymer brushes. When $f_{TOL} < 0.2$, the PS brush swelled very little. In between these two limits, the degree of swelling gradually decreased with decreasing f_{TOL}. This dependency can be rationalized by taking account of mixing and conformational entropies; the former causes brush swelling by osmotic pressure and the latter is responsible for the elastic stress. These two forces are balanced in equilibrium of swelling. The saturated degree of swelling can presumably be attributed to a rapid increase in conformational entropy (and hence extension stress) when the graft chain extends to almost full length.

dx.doi.org/10.1021/ma200340d |*Macromolecules* 2011, 44, 5013–5019

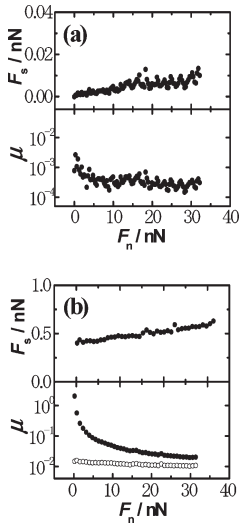

Figure 4. Plots of frictional force F_s and frictional coefficient μ (= F_s/F_n) vs normal load F_n measured at v = 7 μm/s between the PS brushes (samples 2 and 3 against PS-brush modified particle) in solvents with (a) f_{TOL} = 1.0 and (b) f_{TOL} = 0.4. In Figure 4b, the frictional coefficient corrected with adhesion force as $\mu = F_s/(F_n +$ adhesion force in Figure 6) is also plotted (○). The frictional force-curve method (see Experimental Section) with PS-grafted SiP mounted on a rectangular-shaped cantilever was used to measure F_s.

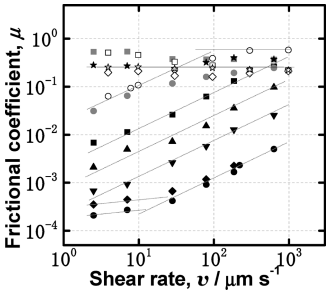

Figure 5. Plot of frictional coefficient μ vs shear velocity v between the PS brushes (sample 2 and 3 against PS-brush modified particle) measured in toluene/2-propanol-mixed solvents at F_n = 20 nN; f_{TOL} = 1.0 (●), 0.7 (♦), 0.6 (▼), 0.5 (▲), 0.4 (■), 0.3 (gray circle), 0.2 (gray square), 0.0 (★) for the force-curve method, and 0.3 (○), 0.2 (□), 0.1 (◊), 0.0 (☆) for the frictional-loop method (see Experimental Section). The PS-grafted SiP mounted on a rectangular-shaped cantilever was used as a probe.

Frictional Property and Mechanism in Mixed Solvents. Parts a and b of Figure 4 show the F_s and μ values of the CPBs of PS against F_n at v = 7 μm/s in solvents with f_{TOL} = 1.0 and 0.4, respectively. At f_{TOL} = 1.0 (Figure 4a), F_s is almost proportional to F_n, giving an almost constant value of $\mu = 2 \times 10^{-4}$, close to the value previously reported for the CPBs of PMMA.[17] At f_{TOL} = 0.4 (Figure 4b), the F_s linearly but not proportionally increased and hence the μ value gradually decreased with increasing F_n. As previously indicated,[39] one of reasons for this is an adhesion force acting as an additional normal load; friction is caused by this adhesion force even when the applied normal load is zero. As plotted by open symbols in Figure 4b, an almost constant μ value was obtained in this friction study when the sum of the applied load and the adhesion force was used as F_n to

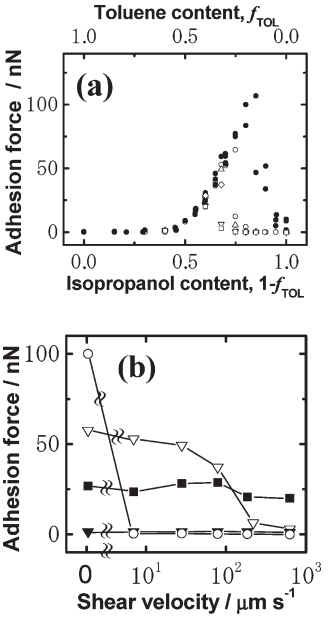

Figure 6. Plots of adhesion force between the PS brushes (samples 2 and 3 against PS-brush modified particle) as a function of (a) solvent composition f_{TOL} and (b) shear velocity v in toluene/2-propanol-mixed solvents: (a) v = 1000 (□), 320 (▽), 100 (◊), 32 (△), 10 (○) 0 (●) μm/s, and (b) f_{TOL} = 0.6(▼), 0.4(■), 0.3(▽), 0.2(○). The PS-grafted SiP mounted on a rectangular-shaped cantilever was used as a probe.

calculate the μ value. In the following section, we will estimate the μ value by correcting the adhesion force.

Figure 5 shows the plot of μ vs v in solvents with different values of f_{TOL}. Under good-solvent conditions, i.e., at f_{TOL} = 1.0 and 0.7, μ increased with increasing v at high regions of v, seemingly giving a constant slope in the logarithmic plot. In lower regions of v, the slope decreased with decreasing v. It is quite interesting that the observed μ value and its corresponding v are very similar to results obtained previously for CPB of PMMA with similar σ^* and M_n. Excellent lubrication common to the CPB (regardless of the kind of polymer chain) under good-solvent conditions is well understood by noninterpenetrating interactions as detailed in our previous publication.[17] With decreasing f_{TOL} and hence decreasing the solvent quality, μ increased in almost all the v regions. It is known that the force-curve method might not be able to adequately measure the frictional force because the strong adhesion force may cause the probe sticking to frictional surface to prevent shear, especially under poor solvent conditions. Therefore, we also measured the frictional force by the friction-loop method with longer shear length (5 μm). Comparing μ data in Figure 5, both of these two methods work well to evaluate the frictional force correctly with little differences in results. Interestingly, the data can be categorized into two regimes as a function of f_{TOL} and v. One is shear-velocity dependent with almost the same slope, and the other has less dependence. The lubrication mechanism for these two regimes can be discussed in terms of the boundary and hydrodynamic lubrications, which were previously proposed for the CPB of PMMA in a good solvent. In order to discuss the interaction between the polymer brushes in both good/nonsolvents, the adhesion force was measured and plotted as a function of f_{TOL} and v in Figure 6.

Boundary Lubrication. Here, we describe the boundary-lubrication regime, in which the load is carried by the physical

dx.doi.org/10.1021/ma200340d |*Macromolecules* 2011, 44, 5013–5019

or chemical properties of confronted surfaces including asperities or adhesiveness rather than those of the lubricant.[40,41] Our previous study on the PMMA brushes in toluene revealed that the degree of interpenetration between graft polymer chains impacts upon the friction;[17] the CPB was demonstrated to have an extremely low value of μ for any applied loads at a low v because the interpenetration was drastically suppressed due to the entropic effect of highly extended polymer chains. The weak v-dependency was previously reported for a system in which the polymer brushes interpenetrate at a faster rate than the applied shear velocity.[42] In this study, a regime with μ on the order of 10^{-4} and a weak v-dependency was also observed at a low v region between the CPBs of PS under good-solvent conditions, i.e., at f_{TOL} = 1.0 and 0.7, where the brush had a highly stretched conformation ~80% of the $L_{c,w}$ (as mentioned above) and little adhesion force (see the data plotted by closed symbols in Figure 6a).

In addition to these cases, a weak v-dependency was also observed in solvents with f_{TOL} lower than 0.2 (Figure 5). The PS-brush layer adopts a glassy state, and can no longer function as an effective lubricant layer. The small v-dependency of μ may be understood by considering Amonton's law, in which the kinetic frictional force between solid surfaces bears no relation to the shear velocity.[43] Figure 3 suggests that under these conditions, the PS brush is less swollen, giving a value of $L_e/L_d - 1$ (the solvent fraction in the brush) less than 0.1 at f_{TOL} = 0.2 and almost zero at f_{TOL} = 0 (pure 2-propanol, nonsolvent). The presence of solvent somehow decreases the glass transition temperature T_g of the polymer due to the reduced barriers for the rotational and transitional motions of chain segments as the described by the following equation,

$$1/T_g = W_1/T_{g1} + W_2/T_{g2} \quad (4)$$

where W is the weight fraction and the subscripts 1 and 2 refer to the polymer and the diluent, respectively.[44−46] Using the T_g data of PS (T_{g1}) as 100 °C[30] and 2-propanol (T_{g2}) as −152 °C,[47] the T_g of the swollen PS brush layer for W_1 = 0.9 and hence W_2 = 0.1 (at f_{TOL} = 0.2) was estimated to be about 30 °C, which is approximately the room temperature at which the friction measurements were conducted. This glassy-state brush layer under poor solvent conditions with f_{TOL} lower than 0.2 should result in a loss in lubricant efficiency.

Figure 6a suggests that the adhesion force remained at ~0 nN for f_{TOL} > 0.7 and then increased with decreasing f_{TOL}, reaching a maximum and suddenly decreasing at a critical value $f_{TOL,c}$. The sudden decrease in adhesion force can be attributed to asperities, i.e., decreasing area of contact due to the glass transition of the polymer-brush layer. Interestingly, the adhesion force followed the same f_{TOL} dependency up to its maximum at $f_{TOL,c}$ independent of v (with and without shearing), while the $f_{TOL,c}$ decreased with increasing v. Of course, the glass transition should be time-dependent. This is consistent from the data obtained at f_{TOL} = 0.3 as shown in Figure 6b; the adhesion force drastically falls at v = 200 μm/s. This is reflected in the data at f_{TOL} = 0.3 in Figure 5, where the μ value increased with increasing v, approaching an almost constant value beyond v = 100 μm/s.

Hydrodynamic Lubrication. We now discuss hydrodynamic lubrication, in which the frictional force is determined by the viscosity of solvent rather than the interactions between surfaces. From the viscosity law, the frictional force in hydrodynamic lubrication can be formulated as follows[48]

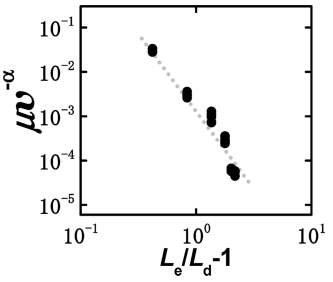

Figure 7. Plot of frictional coefficient reduced by shear velocity with parameter α as a function of degree of swelling $L_e/L_d - 1$ for the data in the regime corresponding to hydrodynamic lubrication.

$$\mu = \beta \cdot v^{\alpha} \quad (5)$$

where α is the parameter representing the shear-flow distribution in a lubricating layer and β is a function of viscosity and the effective thickness of the lubricating layer. This lubrication mechanism is expected to come into play when the shear velocity exceeds a certain value and the friction caused by boundary lubrication is relatively small. The α parameter is unity for Newtonian fluids but usually much smaller for polymer solutions behaving as non-Newtonian fluids,[48] in which the entanglement of polymer chains hinders uniform shear-flow distribution of solvent molecules. The data in Figure 5 except for those in the above-mentioned regime of boundary lubrication behaved in accordance with eq 5. It is notable that the data at different f_{TOL} values ranging from 1.0 to 0.3 can be well fitted by a line with almost the same slope in the double logarithmic plot. An almost constant α value of ca. 0.7 is obtained, even though the degree of swelling changes significantly as shown in Figure 3. Another interesting point is that in those cases, the adhesion force was detected as shown in Figure 6, indicating that the friction caused by this adhesive interaction should be low enough to achieve hydrodynamic lubrication.

The β parameter, corresponding to intercept of the graph in Figure 5 increased with decreasing f_{TOL}, as the above-mentioned fitted line shifted to higher values. This can be explained by the decreasing degree of swelling. In Figure 7, the μ values scaled by $v^{-\alpha}$ (α = 0.7) were replotted in the double logarithmic scale against $L_e/L_d - 1$ as a measure of the degree of swelling. This showed a good linearity, indicating that the β (= $\mu v^{-\alpha}$) parameter was scaled by the degree of swelling, which should result in increasing viscosity in the brush and its thickness. Further investigations are underway to fully characterize this relationship.

Three types of lubricating layers can be proposed for hydrodynamic lubrication: (a) a pure-solvent layer, which is usually assumed for a system between solid surfaces under high shear conditions, (b) the swollen brush or its outermost part with a certain depth from the surface, and (c) mixing. As shown in Figure 6b, a certain amount of adhesion force was observed between the PS-brush surfaces under reciprocal motion. One may suppose that the interaction around the turning points of the reciprocating motion is the origin of this adhesion. However, this possibility was ruled out by the measurement of frictional loop, which detected no enhanced interaction around these points. Thus, the confronted polymer-brush layers interacted with each other even in the regime of hydrodynamic lubrication. In addition to this consideration, the α value was close to unity

when compared with the systems containing polymer solutions. This indicates that the hydrodynamically lubricating layer composed by the CPB caused less hindrance to the shear flow of solvent infiltrating into the brush layer. This might be the characteristic features of the lubrication mechanism of the CPB in addition to the ultralow frictional property. These considerations suggest another method of possible lubrication whereby a pure-solvent layer might be produced between two brush surfaces at much higher shear velocity.

CONCLUSIONS

We have studied the friction/lubrication properties of the CPBs of PS in toluene/2-propanol-mixed solvents using an AFM-colloidal-probe technique. The PS brushes prepared in this study via surface-initiated ATRP were reasonably categorized in the CPB regime, on the basis that the graft density was sufficiently higher than the critical value for the CPB and that the graft chains were highly stretched to almost 80% of the contour length in a good solvent (pure toluene). The degree of swelling of the brush was successfully controlled by varying the solvent composition of toluene/2-propanol mixture.

The μ data as a function of shear velocity and solvent composition (and hence degree of swelling) was divided into two regimes corresponding to different lubrication mechanisms. One is boundary lubrication, in which the chemical or physical property of the outermost surface determines the frictional force. At low shear velocity in toluene-rich solvents, the boundary-lubrication mechanism afforded μ values that are less dependent on shear velocity and are exceptionally small (on the order of 10^{-4}), similar to the previous studies of CPB of PMMA in toluene. This had been ascribed to effective suppression of interpenetration between polymer brushes. Boundary lubrication was also observed in 2-propanol-rich solvents, where the PS-brush layer was in a glassy state with μ on the order of 0.1 independent of shear velocity.

The second mechanism is hydrodynamic lubrication, in which the viscosity resistance owing to the solvent-swollen polymer brush dominates the friction. This was observed in a wide range of solvent compositions except for those in the glassy state. The data in this regime can be described by the relationship $\mu = \beta \cdot v^{\alpha}$. An almost constant value of $\alpha = 0.7$ was obtained and β depended on the solvent composition and was scaled by the degree of swelling. The measurement of the adhesion force revealed that the confronted polymer brushes interacted with each other in this regime, which is different from the usual hydrodynamic lubrication forming a pure-solvent layer. The CPB in solvents would be an efficient lubricating layer presumably because of its high osmotic pressure. This work allows for the design of friction/lubrication-controlled materials by taking advantage of novel properties of the CPBs.

ACKNOWLEDGMENT

This work was partly supported by a Grant-in-Aid for Scientific Research (Grant-in-Aid 17002007 and 21245031) from the Ministry of Education, Culture, Sports, Science, and Technology, Japan.

REFERENCES

(1) Zhang, S. L.; Tsou, A. H.; Li, J. C. M. *J. Polym. Sci., Part B: Polym. Phys.* **2002**, *40*, 1530–1537.
(2) Zappone, B.; Rosenberg, K. J.; Israelachvili., J. *Tribol. Lett.* **2007**, *26*, 191–201.
(3) Hutchings, L. R.; Narrianen, A. P.; Thompson, R. L.; Clarke, N.; Ansari, L. *Polym. Int.* **2008**, *57*, 163–170.
(4) Joanny, J. F. *Langmuir* **1992**, *8*, 989–995.
(5) Klein, J.; Kumacheva, E.; Perahia, D.; Mahalu, D.; Warburg, S. *Faraday Discuss* **1994**, *98*, 173–188.
(6) Grest, G. S. *Curr. Opin. Colloid Interface Sci.* **1997**, *2*, 271–277.
(7) Ndoni, S.; Jannasch, P.; Larsen, N. B.; Almdal, K. *Langmuir* **1999**, *15*, 3895–3865.
(8) Klein, J.; Kumacheva, E.; Mahalu, D.; Perahia, D.; Fetters, L. J. *Nature* **1994**, *370*, 634–636.
(9) Raviv, U.; Giasson, S.; Kampf, N.; Gohy, J. F.; Jerome, R.; Klein, J. *Nature* **2003**, *425*, 163–165.
(10) Muller, M.; Lee, S.; Spikes, H. A.; Spencer, N. D. *Tribol. Lett.* **2003**, *15*, 395–405.
(11) Yan, X. P.; Perry, S. S.; Spencer, N. D.; Pasche, S.; De Paul, S. M.; Textor., M.; Lim, M. S. *Langmuir* **2004**, *20*, 423–428.
(12) Edmondson, S.; Osborne, V. L.; Huck, W. T. S. *Chem. Soc. Rev.* **2004**, *33*, 14–22.
(13) Tsujii, Y.; Ohno, K.; Yamamoto, S.; Goto, A.; Fukuda, T. *Adv. Polym. Sci.* **2006**, *197*, 1–45.
(14) Barbey, R.; Lavanant, L.; Paripovic, D.; Schuwer, N.; Sugnaux, C.; Tugulu, S.; Klok, H. A. *Chem. Rev.* **2009**, *109*, 5437–5527.
(15) Yamamoto, S.; Ejaz, M.; Tsujii, Y.; Matsumoto, M.; Fukuda, T. *Macromolecules* **2000**, *33*, 5602–5607.
(16) Yamamoto, S.; Ejaz, M.; Tsujii, Y.; Fukuda, T. *Macromolecules* **2000**, *33*, 5608–5612.
(17) Tsujii, Y.; Okayasu, K.; Nomura, A.; Ohno, K.; Fukuda, T. Submitted for publication.
(18) Sakata, H.; Kobayashi, M.; Otsuka, H.; Takahara, A. *Polym. J.* **2005**, *37*, 767–775.
(19) Kobayashi, M.; Terayama, Y.; Hosaka, N.; Kaido, M.; Suzuki, A.; Yamada, N.; Torikai, N.; Ishihara, K.; Takahara, A. *Soft Matter* **2007**, *3*, 740–746.
(20) Kobayashi, M.; Takahara, A. *Chem. Rec.* **2010**, *10*, 208–216.
(21) Ishikawa, T.; Kobayashi, M.; Takahara, A. *ACS Appl. Mater. Interfaces* **2010**, *2*, 1120–1128.
(22) Bhushan, B. *Introduction to Tribology*; John Wiley & Sons Inc: New York, 2002.
(23) Ohno, K.; Morinaga, T.; Koh, K.; Tsujii, Y.; Fukuda, T. *Macromolecules* **2005**, *38*, 2137–2142.
(24) Husseman, M.; Malmstrom, E. E.; McNamara, M.; Mate, M.; Mecerreyes, D.; Benoit, D. G.; Hedrick, J. L.; Mansky, P.; Huang, E.; Russell, T. P.; Hawker, C. J. *Macromolecules* **1999**, *32*, 1424–1431.
(25) Von Werne, T.; Patten, T. E. *J. Am. Chem. Soc.* **1999**, *121*, 7409–7410.
(26) Pyun, J.; Jia, S.; Kowalewski, T.; Patterson, G. D.; Matyjaszewski, K. *Macromolecules* **2003**, *36*, 5094–5104.
(27) Blomberg, S.; Ostberg, S.; Harth, E.; Bosman, A. W.; Van Hor, B.; Hawker, C. J. *J. Polym. Sci., Part A: Polym. Sci.* **2002**, *40*, 1309–1320.
(28) Tsujii, Y.; Ejaz, M.; Sato, K.; Goto, A.; Fukuda, T. *Macromolecules* **2001**, *34*, 8872–8878.
(29) Morinaga, T.; Ohkura, M.; Ohno, K.; Tsujii, Y.; Fukuda, T. *Macromolecules* **2007**, *40*, 1159–1164.
(30) Brandrup, J.; Immergut, E. H.; Grulke, E. A., Eds.; *Polymer Handbook*; John Wiley & Sons Inc: New York, 1999.
(31) Ducker, W. A.; Senden, T. J.; Pashley, R. M. *Langmuir* **1992**, *8*, 1831–1836.
(32) Ogletree, D. F.; Carpick, R. W.; Salmeron, M. *Rev. Sci. Intrum.* **1996**, *67*, 3298–3306.
(33) Meyer, G.; Amer, N. M. *Appl. Phys. Lett.* **1990**, *57*, 2089–2091.
(34) Green, C. P.; Lioe, H.; Cleveland, J. P.; Proksch, R.; Mulvaney, P.; Sader, J. E. *Rev. Sci. Instrum.* **2004**, *75*, 1988–1966.
(35) Taunton, H. J.; Toprakcioglu, C.; Fetters, L. J.; Klein, J. *Macromolecules* **1990**, *23*, 571–580.
(36) Courvoisier, A.; Isel, F.; Francois, J.; Maaloum, M. *Langmuir* **1998**, *14*, 3727–3729.

(37) Oshea, S. J.; Welland., M. E.; Rayment, T. *Langmuir* **1993**, *9*, 1826–1835.
(38) Shim, D. F. K.; Cates, M. E. *J. Phys. (Paris)* **1989**, *50*, 3535–3551.
(39) Butt, H. J.; Kappl, M. *Surface and Interfacial Forces*; Wiley-VCH: Weinheim, Germany, 2006.
(40) Kaneko, D.; Oshikawa, M.; Yamaguchi, T.; Gong, J. P.; Doi, M. *J. Phys. Soc. Jpn.* **2007**, *76*, 043601.
(41) Wang, W. Z.; Hu, Y. Z.; Liu, Y. C.; Wang, H. *Tribol. Int.* **2007**, *40*, 687–693.
(42) Tadmor, R.; Janik, J.; Klein, J.; Fetters, L. J. *Phys. Rev. Lett.* **2003**, *91*, 115503.
(43) Amonton, G. *Mem. Acad. R. A* **1699**, 275–282.
(44) Fox, T. G. *Bull. Am. Phys. Soc.* **1956**, *1*, 123.
(45) Nielson, L. E. *Mechanical Properties of Polymers*; Reinhold: New York, 1962.
(46) Sung, Y. K.; Gregonis, D. E.; Russell, G. A.; Andrade, J. D. *Polymer* **1978**, *19*, 1362–1363.
(47) Faucher, J. A.; Koleske, J. V. *Phys. Chem. Glasses* **1966**, *7*, 202.
(48) Barnes, H. A.; Hutton, J. F.; Walters, K. *An Introduction to Rheology*; Elsevier: Amsterdam, 1989.